Macromolecules
ARTICLE

Macromolecules **2010**, *43*, 4023–4031 **4023**
DOI: 10.1021/ma1006039

Termination and Transfer Kinetics of Butyl Acrylate Radical Polymerization Studied via SP-PLP-EPR

Johannes Barth, Michael Buback,* Pascal Hesse, and Tatiana Sergeeva

Institute for Physical Chemistry, University of Göttingen, Tammannstrasse 6, D-37077 Göttingen, Germany

Received February 3, 2010; Revised Manuscript Received March 19, 2010

ABSTRACT: Butyl acrylate (BA) solution polymerization (1.5 M in toluene) was investigated via single-pulse pulsed laser polymerization in conjunction with electron paramagnetic resonance spectroscopy (SP-PLP-EPR) with emphasis on the termination and transfer kinetics of the system in which two distinctly different types of radicals, secondary chain-end radicals (SPRs) and midchain radicals (MCRs), are present. MCRs are produced by intramolecular hydrogen transfer (backbiting). They may react back to SPRs by monomer addition. The evolution of SPR and MCR concentrations after photoinitiation with an intense laser pulse was measured via highly time-resolved EPR at temperatures between −40 and +60 °C. At very low temperatures the MCR concentration is negligible, enabling the chain-length-dependent rate coefficient of SPR termination, $k_t^{ss}(i,i)$, to be directly determined. At higher temperatures it was necessary to use PREDICI simulation of the radical concentration vs time traces, a process which yields the chain-length-dependent rate coefficient of SPR termination for monomeric radicals, $k_t^{ss}(1,1)$, as well as the rate coefficients for backbiting, k_{bb}, for monomer addition to an MCR, k_p^t, and for SPR-MCR cross-termination, k_t^{st}. The composite model adequately represents $k_t^{ss}(i,i)$, with the power-law exponents $\alpha_s = 0.85 \pm 0.09$ and $\alpha_l = 0.16 \pm 0.07$ for short-chain and long-chain radicals, respectively, and a crossover chain length between short-chain and long-chain behavior at around $i_c = 30$. The activation energy for both $k_t^{ss}(1,1)$ and $k_t^{st}(1,1)$ is found to be as one would expect for translational diffusion of small molecules.

Introduction

Radical polymerization of acrylates has been studied extensively over the past 50 years.[1] Despite the enormous industrial interest, kinetics and mechanisms of this reaction are not yet fully understood. As was first reported by Scott and Senogles,[2−4] acrylate kinetics differ from ideal behavior. The dependence of polymerization rate on monomer concentration is unusual in that, depending on monomer concentration, reaction orders between 1.4 and 1.8 are observed.[5−8] Measurement of accurate rate coefficients for acrylate radical polymerization is further complicated by the partial failure of the IUPAC-recommended pulsed laser polymerization−size exclusion chromatography (PLP-SEC) method to yield propagation rate coefficients, k_p.[9,10] In PLP-SEC studies above 20 °C, unstructured polymer molecular weight distributions (MWDs) are obtained, which are not suitable for k_p determination,[11] when laser pulse repetition rates below 100 Hz were applied.[12]

It is now generally accepted that intramolecular chain transfer, in particular the 1,5-hydrogen shift, is responsible for these difficulties.[11,13−15] This so-called backbiting reaction, by which a secondary radical is transformed into a tertiary one, was suggested in analogy to the backbiting process in ethene polymerization, where the driving force comes from the transformation of a primary chain-end radical into a secondary midchain radical.[16,17] The occurrence of backbiting in acrylate polymerization has been proven by EPR.[18−21] In principle, also intramolecular chain transfer to a remote chain position and intermolecular chain transfer to another polymer molecule may take place.[1] These latter processes are however not significant in butyl acrylate (BA) polymerization at low and moderate degrees of monomer conversion.[22−24]

*Corresponding author: e-mail mbuback@gwdg.de; Fax +49 551 393144.

The relevant steps of BA radical polymerization up to moderately high temperatures are summarized in Scheme 1. Tertiary midchain radicals (MCRs) are produced by backbiting reactions of secondary propagating chain-end radicals (SPRs). Monomer addition to an MCR produces an SPR under simultaneous formation of a short-chain branch. SPRs rapidly propagate and undergo backbiting or termination with another SPR or an MCR. Propagation from an MCR is by ∼2 orders of magnitude slower than the one from an SPR. Also, MCR homotermination is slower than SPR homotermination. Termination processes in BA polymerization most likely occur by combination.[25]

Several pulsed-laser-assisted techniques have recently been applied for measuring rate coefficients of BA polymerization. The propagation rate coefficient of SPRs, k_p, was determined by PLP-SEC at low temperatures and high pulse repetition rates.[11,12] The backbiting rate coefficient, k_{bb}, was obtained by frequency-tuned pulsed laser polymerization in conjunction with size-exclusion chromatography (ft-PLP-SEC)[25] and also via ^{13}C NMR analysis of the branching level in polyBA.[27] The MCR propagation rate coefficient, k_p^t, has also been determined by two independent methods: (a) by ft-PLP-SEC experiments[25] under the so-called long chain approximation (LCA), which assumes that the equilibrium between SPRs and MCRs is essentially determined by backbiting of SPRs and propagation of MCRs, with negligible contribution by termination; (b) relative concentrations of SPRs and MCRs are directly measured via EPR under conditions where the LCA approximation holds, meaning that the ratio directly yields k_p^t in the event that k_{bb} is known.[22] The LCA approximation may not hold at temperatures below 50 °C. Although the k_p^t data deduced from the two methods show close agreement between +50 and +70 °C, a further independent access to k_p^t appears desirable.

Published on Web 04/16/2010

Scheme 1. Basic Kinetic Scheme for BA Polymerization at Low Degrees of Monomer Conversion and Temperatures below 80 °C, Where β-Scission of MCRs May Be Ignored[24,26] [a]

initial propagation step

$$R_0 + M \xrightarrow{k_i} SPR_1 \quad (a)$$

propagation

$$SPR_i + M \xrightarrow{k_p} SPR_{i+1} \quad (b)$$

backbiting

$$SPR_i \xrightarrow{k_{bb}} MCR_i \quad (c)$$

monomer addition to mid-chain radical

$$MCR_i + M \xrightarrow{k_p^t} SPR_{i+1} + (SCB) \quad (d)$$

chain transfer to monomer

$$SPR_i + M \xrightarrow{k_{tr,M}^s} P_i + SPR_1 \quad (e)$$

$$MCR_i + M \xrightarrow{k_{tr,M}^t} P_i + SPR_1 \quad (f)$$

termination by combination

$$SPR_i + SPR_j \xrightarrow{k_t^{ss}} P_{i+j} \quad (g)$$

$$SPR_i + MCR_j \xrightarrow{k_t^{st}} P_{i+j} \quad (h)$$

$$MCR_i + MCR_j \xrightarrow{k_t^{tt}} P_{i+j} \quad (i)$$

[a] Not included is chain-length-dependent propagation and termination by disproportionation.

The knowledge of individual termination rate coefficients (see Scheme 1) is less advanced. The RAFT-SP-PLP and the RAFT-CLD-T methods have been applied toward the analysis of chain-length-dependent termination (CLD-T) in BA polymerization.[28−33] The rate coefficients obtained by these strategies are in reasonable agreement. A drawback of this data is that effective rate coefficients are measured which provide no access to the individual coefficients for termination, e.g., of SPR-SPR (k_t^{ss}) and SPR-MCR (k_t^{st}) species. Furthermore, no temperature dependence for k_t^{ss} has been determined so far. An attempt to estimate chain-length averaged $\langle k_t^{st} \rangle$ and $\langle k_t^{tt} \rangle$ was made in ref 34. Mean values of the termination rate coefficients $\langle k_t^{ss} \rangle$, $\langle k_t^{st} \rangle$, and $\langle k_t^{tt} \rangle$ were estimated from the lumped parameters $k_t^{ss}/(k_p^s)^2$, $\theta_1 = (2k_t^{st}k_{bb})/(k_t^{ss}k_p^t)$, and $\theta_2 = (k_t^{tt}/k_t^{ss})/(k_{bb}/k_p^t)^2$ obtained by analysis of experimental rate data for stationary BA polymerization at 50 °C[8,35] and by assuming the activation energy of the three termination rate coefficients to be identical and to be given by the value deduced from SP-PLP-NIR experiments.[36]

Direct information on termination kinetics comes from the measurement of radical concentration vs time profiles under nonstationary but well-defined reaction conditions. The SP-PLP-EPR method should be perfectly suited for such detailed studies. Initiation occurs by a laser single pulse (SP) which almost instantaneously decomposes a photoinitiator. The resulting radicals induce pulsed laser polymerization (PLP). The evolution of radical concentration after firing the SP is monitored by time-resolved EPR. As the size of the growing (and terminating) radicals increases with time t after applying the SP, the method provides easy access to chain-length-dependent rate coefficients, $k_t(i,i)$, for termination of two radicals of (almost) identical chain length. The SP-PLP-EPR technique was first applied to determine $k_t(i,i)$ of slowly terminating polymerization systems, such as dodecyl methacrylate,[37,38] cyclohexyl methacrylate,[38] benzyl methacrylate,[38] and dibutyl itaconate.[39] More recently, monomers that exhibit faster termination, such as *n*-BMA and *tert*-BMA[40] as well as MMA,[41] have been investigated.

The aim of the present study was to apply highly time-resolved EPR spectroscopy toward the analysis of the complicated BA system, in which two types of radicals, SPRs and MCRs, are present which both may be monitored by time-resolved EPR. To reduce polarity, the SP-PLP-EPR experiments have been carried out for BA polymerization in toluene solution. The so-called composite model (eq 1) will be used for representation of the chain-length dependence of $k_t(i,i)$ of SPR radicals.[42,43] This model assumes a power-law expression for k_t with the exponent being different for short-chain and long-chain radicals, α_s and α_l, respectively. The transition between the two regimes occurs at the crossover chain length i_c:

$$\begin{aligned} k_t(i,i) &= k_t(1,1)i^{-\alpha_s} \qquad i \le i_c \\ &= k_t(1,1)i_c{}^{-\alpha_s+\alpha_l}i^{-\alpha_l} = k_t^0 i^{-\alpha_l} \qquad i > i_c \end{aligned} \quad (1)$$

$k_t(1,1)$ is the termination rate coefficient of two radicals of chain length unity, whereas k_t^0 is the termination rate coefficient of two hypothetical radicals of chain length unity which terminate by segmental diffusion, a process characteristic of long-chain radicals.

The composite-model parameters may be deduced from linear fitting of $\log(c_R^0/c_R - 1)$ vs $\log t$ for the regimes of short-chain (eq 2) and long-chain radicals (eq 3)

$$\frac{c_R^0}{c_R(t)} - 1 = \frac{2k_t^{1,1}c_R^0 t_p{}^{\alpha_s}}{1-\alpha_s}t^{1-\alpha_s} \qquad \text{for } i \le i_c \quad (2)$$

and

$$\frac{c_R^0}{c_R(t)} - 1 = \frac{2k_t^0 c_R^0 t_p{}^{\alpha_l}}{1-\alpha_l}t^{1-\alpha_l} \qquad \text{for } i > i_c \quad (3)$$

with c_R^0 being the maximum initial radical concentration produced by the laser pulse and $t_p = (c_M k_p)^{-1}$ the time interval required for a single propagation step. Equations 2 and 3 are based on the correlation $i = k_p c_M t$ which is however not adequate at very small chain lengths and, as suggested by Smith and Russell,[43] needs to be replaced by the physically more reasonable relation $i = k_p c_M t + 1$. This modification leads to eq 4, which has been used for deducing α_s and $k_t(1,1)$ for the short-chain radicals:

$$\frac{c_R^0}{c_R(t)} - 1 = \frac{2k_t^{1,1}c_R^0((k_p c_M t+1)^{1-\alpha_s}-1)}{k_p c_M(1-\alpha_s)} \qquad \text{for } i \le i_c \quad (4)$$

The exponent α_s is expected to be in the range 0.5−1.0 with the lower and upper limits being associated with center-of-mass diffusion of random coils and rodlike chains, respectively.[44−46] Radicals of chain lengths above i_c may get entangled and thus may experience considerably increased contact times for segmental diffusion and subsequent termination.

Mean-field theory predicts $\alpha_l = 0.16$ for radicals at the end of long chains in a good solvent.[47−49] So far, mostly nonstationary SP-PLP-NIR-RAFT[28−30] and stationary RAFT-CLD-T[31−33] techniques have been used to derive power-law exponents and crossover chain lengths according to the composite model. The SP-PLP-EPR method has the advantage of being applicable to polymerizing systems without a RAFT agent being present. This is an advantage because a RAFT agent may affect kinetics,[40] e.g., by an impact of the RAFT equilibrium and by rate retardation effects associated with RAFT mediating species. Moreover, the RAFT-CLD-T method requires the knowledge of initiator concentration, initiator efficiency, and initiator decomposition rate

coefficient, all as a function of conversion, for deducing chain-length-dependent termination coefficients from the primary experimental data. The SP-PLP-EPR experiment may be carried out, and the chain-length dependence of k_t thus may be mapped out at any time during the course of polymerization up to high conversion. Other than with the RAFT-mediated techniques, the termination rate is not studied under conditions of simultaneous increase of conversion and chain length. The most important and unique advantage of SP-PLP-EPR, however, consists in the direct access to individual concentration vs time traces for SPRs and MCRs. As backbiting is negligible at temperatures below −40 °C,[13,22] BA polymerization occurs in a less complicated way under such conditions, and the termination kinetics of SPRs may be elucidated from SP-PLP-EPR without interference from MCRs. Along these lines, α_s, α_l, and i_c will first be determined from separate low-temperature SP-PLP-EPR experiments. The so-obtained composite-model parameters will be assumed to hold at higher temperature. The stepwise procedure of combining EPR experiments at low and high temperature is advantageous for improving the quality by which α_s, α_l, i_c, $k_t(1,1)$, k_{bb}, k_p^t, and k_t^{st} may be deduced from experimental radical concentration vs time traces.

Experimental Section

The experimental setup has been previously described.[40] Briefly, a Bruker Elexsys E 500 series CW-EPR spectrometer was used for the experiments. Typical EPR parameter settings were 3 G field modulation amplitude, 100 kHz field modulation frequency, 10 mW microwave power, and a time constant of 0.01 ms. Sample volumes of 0.20 mL were filled into quartz tubes of 5 mm o.d. and 4 mm i.d. The tubes were fitted into the resonator cavity equipped with a grid through which the sample was irradiated by a COMPex 102 excimer laser (Lambda Physik) operated on the XeF line (351 nm) at laser energies between 10 and 80 mJ/pulse. The EPR spectrometer and the laser source were synchronized by a pulse generator (Scientific Instruments 9314). Temperature control in the range −40 to +60 °C was achieved via an ER 4131VT unit (Bruker) by purging the sample cavity with nitrogen.

Butyl acrylate (BA) (> 99.5%, stabilized with hydroquinone monomethyl ether, Fluka) was purified by passing through a column filled with inhibitor remover (Aldrich). The solvent toluene (99.5%, Fluka) was used without further purification. Dissolved oxygen was removed by several freeze−pump−thaw cycles. The photoinitiator α-methyl-4(methylmercapto)-α-morpholinopropiophenone (MMMP, 98%, Aldrich) was used as received at initial concentrations of about 1.6×10^{-2} mol L^{-1}. MMMP was added to the degassed monomer in a glovebox under an argon atmosphere. The EPR tube was sealed with a plastic cap and with Parafilm and was protected from light prior to PLP.

Results and Discussion

Prior to an SP-PLP-EPR experiment, the full EPR spectrum is recorded under pseudostationary PLP conditions by signal channel (SC) detection. This spectrum serves for optimization of modulation amplitude and microwave energy (to avoid saturation) and for identification of the peak maximum positions to be used in the time-resolved measurement. Shown in Figure 1 is an example of such an EPR spectrum, which was recorded during PLP of BA at a laser pulse repetition rate of 20 Hz and 0 °C. A short sweep time of 10.5 s was chosen to avoid significant monomer conversion prior to the actual SP experiment.

Periodic laser pulse initiation enormously facilitates the assignment of individual EPR lines to SPR and MCR species. As has been detailed elsewhere,[50] SPRs are identified with radical species which oscillate with pulse laser repetition rate. The results of the component analysis of the full EPR spectrum into an SPR four-line spectrum and an MCR seven-line spectrum, represented by the dashed black line and the full gray line, respectively, are shown in Figure 2b. For representation of the EPR contour within an extended temperature range it is recommendable to include a third EPR component, which is assigned to MCR species with restricted rotational mobility.[22] The contribution of this third component, which behaves kinetically identically to the MCR seven-line component, is pronounced at intermediate temperatures around 10 °C. At low temperatures, e.g., around

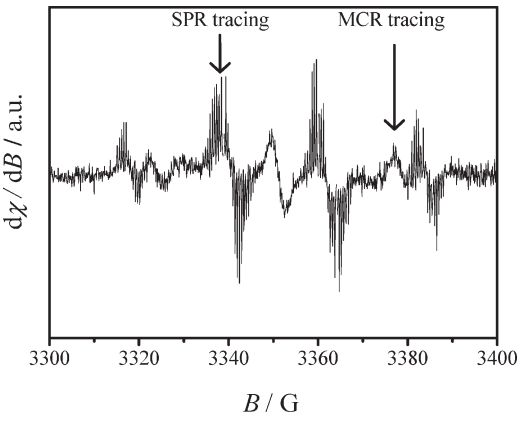

Figure 1. EPR spectrum recorded during laser-initiated polymerization, with pulse repetition rate 20 Hz, of butyl acrylate (1.5 M in toluene) at 0 °C. The SPR lines oscillate with pulsed laser repetition rate due to fast buildup and termination of these chain-end radicals. The field positions for the individual monitoring of SPR and of MCR radicals in the SP-PLP-EPR experiments are indicated by arrows.

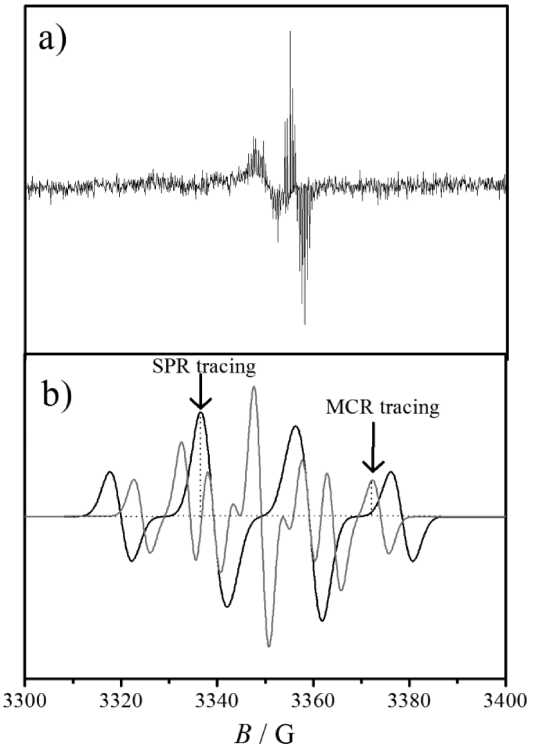

Figure 2. (a) EPR spectrum taken during pulsed-laser irradiation of the photoinitiator MMMP, dissolved in deoxygenized toluene in the absence of BA. (b) Simulated EPR spectra for SPRs (black line) and MCRs (gray line) using the hyperfine coupling constants and line widths reported in ref 13. The field positions for monitoring individual radical species in the SP-PLP-EPR experiments are indicated by the arrows. The EPR intensity vs time traces recorded at the particular SPR position are identical to the ones measured at the lowest SPR field component.

−40 °C, MCRs are not present to any significant extent, whereas at and above 30 °C, the MCR component with restricted rotational mobility plays no major role. Thus, within the present study, only a two-component system, composed of SPRs and of one type of MCR, is taken into account. As outlined by Figure 2a, the intense central band is not best suited for MCR detection because of an overlap with EPR bands due to primary radical fragments produced by laser-induced decomposition of the photoinitiator MMMP in toluene. Almost the same spectrum has been detected for MMMP irradiation in benzene, indicating that no benzyl radicals are produced in our BA/toluene system.

Quantitative Determination of Radical Concentrations. Deducing absolute radical concentrations from time-resolved EPR experiments at constant magnetic field requires a three-step calibration procedure: (a) of the double integral of the entire EPR spectrum against a reference radical concentration, (b) of the EPR intensity at a given field position against the double integral, and (c) of the sensitivity of the detector used for the time-resolved experiment against the sensitivity of the detector used for CW detection. The procedure has been carried out in an analogous fashion as described for butyl methacrylate (BMA) polymerization.[40] The situation with BMA is less complicated in that only one type of radical is present, whereas two types of radicals need to be quantitatively monitored in the case of BA. Thus, as an additional piece of information, the fraction of each radical species with respect to overall acrylate radical content needs to be known for the polymerization temperature, initiation rate, and monomer concentration at which the time-resolved experiment is carried out. This information has already been determined by linear demixing of the superimposed experimental EPR two-component spectra.[13,22]

The concentrations of butyl acrylate MCRs and SPRs are obtained via eqs 5 and 6, respectively:

$$c_{\mathrm{MCR}}(t) = h_{\mathrm{a}} h_{\mathrm{b}} h_{\mathrm{c,MCR}} x_{\mathrm{MCR}} I_{\mathrm{FD}}(H_{\mathrm{x,MCR}})(t) \qquad (5)$$

$$c_{\mathrm{SPR}}(t) = h_{\mathrm{a}} h_{\mathrm{b}} h_{\mathrm{c,SPR}} x_{\mathrm{SPR}} I_{\mathrm{FD}}(H_{\mathrm{x,SPR}})(t) \qquad (6)$$

The mole fractions, x_{MCR} and x_{SPR}, add up to unity:

$$x_{\mathrm{SPR}} = (1 - x_{\mathrm{MCR}}) \qquad (7)$$

The proportionality constants h_{a}, h_{b}, $h_{\mathrm{c,MCR}}$, and $h_{\mathrm{c,SPR}}$ are obtained from the slopes of linear fits associated with the calibration procedures (a) to (c). $I_{\mathrm{FD}}(H_{\mathrm{x,MCR}})$ is the EPR signal at the constant magnetic field position $H_{\mathrm{x,MCR}}$ with the EPR intensity being entirely due to MCRs. $I_{\mathrm{FD}}(H_{\mathrm{x,MCR}})$ is measured via the fast-digitizing detector (FD) after applying a laser single pulse. $I_{\mathrm{FD}}(H_{\mathrm{x,SPR}})$ and $H_{\mathrm{x,SPR}}$ are the corresponding SPR quantities.

MCR and SPR Concentration Traces after Single-Pulse Initiation. Shown in Figure 3 is the time evolution of SPR concentration, c_{SPR}, after single pulse initiation at $t = 0$ for 0, 30, and 60 °C. The first SPR species are formed by monomer addition, with the rate coefficient, k_{i}, to primary photoinitiator-derived radicals. As k_{i} is assumed to be well above k_{p}, the maximum in c_{SPR} is reached immediately after applying a laser pulse; i.e., the initial increase in c_{SPR} is too fast as to be quantitatively measured with the currently available time resolution of our SP-PLP-EPR experiment. The intense laser pulse at $t = 0$ distorts the EPR signal for a few microseconds,[51] which forecloses the exact measurement of the initial c_{SPR}. The decrease in c_{SPR} with time t after pulsing is caused by both termination and backbiting. The

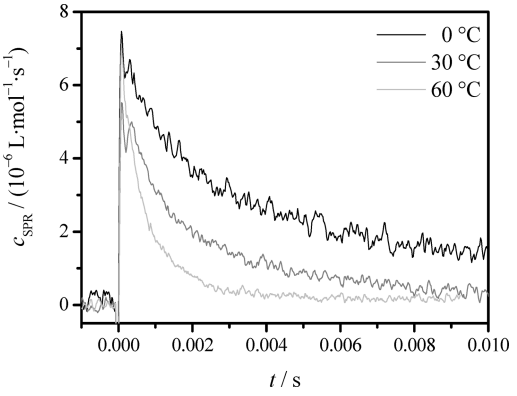

Figure 3. Variation with time t (after applying a laser single pulse at $t = 0$) of SPR concentration, c_{SPR}, for BA polymerizations (1.5 M in toluene) at three temperatures with MMMP acting as the photoinitiator. The concentration is monitored at the constant magnetic field strength indicated by the arrow for SPRs in Figures 1 and 2b. The double-peak contour at very small t is due to an artifact associated with laser pulsing.[51]

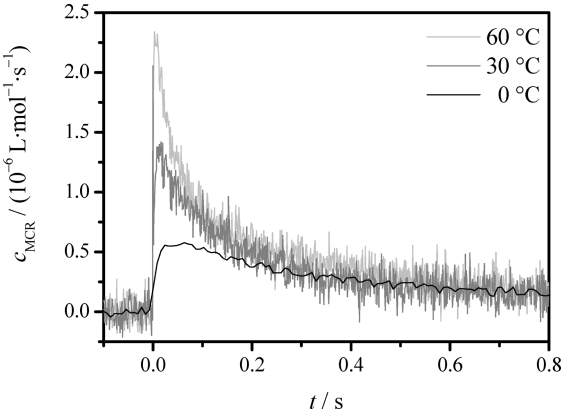

Figure 4. Variation with time t (after applying a laser single pulse at $t = 0$) of MCR concentration, c_{MCR}, for BA polymerizations (1.5 M in toluene) at three temperatures with MMMP acting as the photoinitiator. The concentration is monitored at the constant magnetic field strength indicated by the arrow for MCRs in Figures 1 and 2b. The curve for 0 °C was measured with a lower time resolution as compared to the curves recorded at higher temperature.

dominant reaction at small t is SPR-SPR termination, as both c_{SPR} and $k_{\mathrm{t}}^{\mathrm{ss}}$ are high. SPR-MCR termination becomes significant at high temperatures and longer time intervals after applying the pulse ($t > 0.01$ s) when a considerable concentration of MCRs is present. The larger scatter in signal-to-noise of the lower temperature SPR traces in Figure 3 is due to a smaller number of signals having been coadded.

Figure 4 shows MCR traces measured during SP-PLP-induced polymerizations of BA (1.5 mol L^{-1} in toluene) at 0, 30, and 60 °C. The slope of the $c_{\mathrm{MCR}}(t)$ curves during MCR buildup increases toward higher temperature, as k_{bb} becomes larger. Also, the maximum in c_{MCR} increases with temperature. Only up to 5% of the SPRs are transformed into MCRs at 0 °C, whereas this number increases to 25% at 60 °C. Comparison of the abscissa scales in Figures 3 and 4 tells that MCRs are far more long-lived than SPRs. The maximum in $c_{\mathrm{MCR}}(t)$ reflects the rate of MCR formation, by backbiting, being identical to the sum of the rates of MCR loss by SPR-MCR termination, MCR-MCR termination, and monomer addition to the MCR. In the initial time period SPR-MCR termination is dominant. Toward larger t, the

impact on $c_{MCR}(t)$ of MCR-MCR termination and of propagation from MCRs becomes increasingly important.

Kinetic Analysis of SPR and MCR Concentration vs Time Profiles. The concentration profiles of the two types of radicals are affected by an extended set of individual reactions with mostly unknown rate coefficients (see Scheme 1). The complex interplay between the three types of termination processes, with rate coefficients k_t^{ss}, k_t^{st}, and k_t^{tt}, and the two "transfer" steps between the SPRs and MCRs, with rate coefficients k_{bb} and k_p^t, respectively, poses significant problems toward deducing individual rate coefficients from measured SPR and MCR concentration vs time profiles. To reduce complexity, the kinetic analysis has been performed in a stepwise fashion. First, the kinetics of SPRs are analyzed by carrying out time-resolved experiments at fairly low temperature, where the concentration of MCRs is negligible. Analysis of SPR kinetics yields the termination kinetics of SPRs, i.e., the exponents associated with their short-chain and long-chain behavior together with the crossover chain length. This part of the analysis closely resembles the procedure selected for bulk polymerization of methacrylates, where, irrespective of reaction temperature, only one type of propagating and terminating radical is present.[37−41] The parameters for SPRs are implemented into the kinetic analysis at higher temperature, e.g., between 0 and 60 °C, where the concentration vs time traces of both radicals, SPRs and MCRs, are measured via time-resolved EPR. Simultaneous analysis of the radical concentration profiles may be carried out using the simulation software PREDICI together with the kinetic scheme presented above (Scheme 1).

The two-step procedure was difficult to be applied between −40 and 0 °C, where backbiting occurs to such an extent that MCR formation cannot be ignored. On the other hand, the MCR signal is too weak as to be reliably measured and analyzed for k_{bb} and k_p^t.

Termination Kinetics of BA Polymerization in Toluene Solution at −40 °C. At −40 °C, the MCR content is negligibly low under stationary conditions.[13] With SP-PLP initiation, MCR formation should be even smaller because of the missing buildup of a pseudostationary tertiary radical concentration. The SPR concentration vs time curves are analyzed by plotting $\log(c_R^0/c_{SPR} - 1)$ vs $\log t$. According to eqs 2 and eq 3, two linear regimes should intersect in the crossover region at t_c, which time after pulsing directly yields the crossover chain length i_c by using the relation $i = k_p c_M t + 1$. The propagation rate coefficient was taken from ref 12. Linear fitting for the chain-length region $i > i_c$ yields α_l. As discussed above and in refs 38 and 40, the additional composite model parameters, α_s and $k_t^{ss}(1,1)$, are found from nonlinear fitting of the SPR concentration vs t data for the short-chain regime to eq 4. The parameter values for α_s, α_l, and i_c from analysis at −40 °C are assumed to also hold at higher temperature, which hypothesis appears to be reasonable because of the clear physical meaning behind these parameters: The exponent α_s is associated with the increase in hydrodynamic radius toward higher SPR chain length. The crossover chain length i_c refers to the SPR size beyond which the radicals start to get entangled and form longer-lived contact pairs. The size of the exponent α_l is given by the shielding of radical functionality by the chain segments within the long-lived contact pairs. The assumption of temperature-independent α_s, α_l, and i_c values is supported by recent SP-PLP-EPR studies into chain-length-dependent termination, in which no temperature effect on any of these three parameters has been observed.[37−41] Linear double-log fits to eqs 2 and 3 of $c_{SPR}(t)$ at −40 °C are shown in Figure 5.

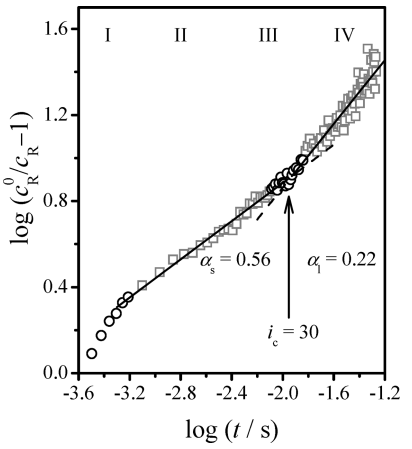

Figure 5. Linear fitting of $c_R(t)$ data from SP-PLP-EPR experiments on BA (1.5 M in toluene) at −40 °C. The experimental data are plotted as $\log(c_R^0/c_R - 1)$ vs $\log t$, where t is the time after laser pulsing. The full lines show the linear fits to the data in the short-chain regime ($3 < i < 25$) in segment II and the long-chain regime ($i > 40$) in segment IV, respectively. The SP-PLP-EPR data were taken at monomer conversions below 10%.

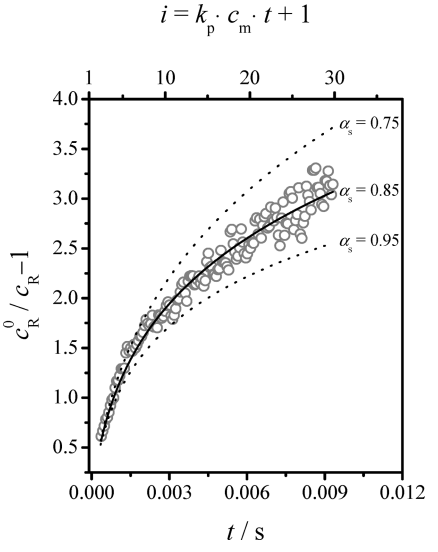

Figure 6. Nonlinear fitting to eq 4 of $c_{SPR}(t)$ data from SP-PLP-EPR experiments on BA (1.5 M in toluene) at −40 °C. The data refers to chain lengths up to the crossover chain length $i_c = 30$.

The crossover chain length i_c is obtained from the intersection of the straight line fits to be $i_c = 30 \pm 5$ (segment III in Figure 5). The exponent α_l is deduced from the slope of the straight line fit to the data for larger chain lengths (segment IV in Figure 5). The $c_R(t)$ data at short chain lengths (segments I and II in Figure 5) are analyzed by nonlinear fitting to eq 4. Given in Figure 6 is the associated plot, which refers to a short-chain exponent of $\alpha_s = 0.85$ and to $k_t^{ss}(1,1) = 1.65 \times 10^8$ L mol^{-1} s^{-1}. To illustrate the accuracy by which α_s may be determined, fitting results (dotted lines) are included in Figure 6 for $\alpha_s = 0.75$ and $\alpha_s = 0.95$.

The composite model parameters α_s, α_l, and i_c are listed in Table 1. The value for i_c is in close agreement with the number deduced from two completely different techniques which are both based on using RAFT agents for controlling radical chain length.[30] The same is true for α_l which value, in addition, agrees within experimental accuracy with the theoretically predicted value of $\alpha_l = 0.16$.[47−49] This theoretical value turns out to provide a slightly better fit of the radical

Table 1. Composite Model Parameters for Termination Kinetics in BA Solution Polymerization (1.52 M in Toluene) at −40 °C

$k_t^{ss}(1,1)/(\text{mol L}^{-1}\text{ s}^{-1})$	α_s	α_l	i_c
$(1.65 \pm 0.50) \times 10^8$	0.85 ± 0.09	0.22 ± 0.07	30 ± 5

concentration vs time profiles measured at polymerization temperatures above 0 °C. Thus, $\alpha_l = 0.16$ has been used for the fitting at higher temperatures rather than the primary experimental value of $\alpha_l = 0.22$ (see Table 1). The α_s value is below the experimental numbers deduced from RAFT-mediated techniques, where short-chain exponents exceeding unity have been found.[30,33,52] Such high values of $\alpha_s > 1$ are difficult to be interpreted. It is possible they arose as artifacts from tertiary radicals being present, a possibility that has deliberately been excluded in the present work. Moreover, cross-termination between SPRs and intermediate radicals is not taken into account in RAFT-mediated experiments. That α_s is below unity gives additional credit to the method presented here. The size of α_s will be further discussed below.

Termination and Transfer Kinetics of BA Polymerization between 0 and +60 °C. The kinetics of BA solution polymerization between 0 and 60 °C were analyzed via iterative parameter refinement using PREDICI modeling of the measured SPR and MCR concentration vs time traces. The concentration of primary radicals produced by the laser single pulse, c_R^0, is estimated by back-extrapolation of measured $c_{SPR}(t)$ toward $t = 0$. The termination rate coefficient of two SPRs of chain length unity, $k_t^{ss}(1,1)$, is found from the SPR trace by fitting the SPR concentration vs time trace in the period shortly after pulsing where backbiting has a minor impact on c_{SPR}. The parameters $k_t^{st}(1,1)$, k_{bb}, and k_p^t are deduced from both the measured SPR and MCR concentration vs time traces.

The chain-length dependence of cross-termination has not been studied in any detail so far. Simulation of our experimental data suggests that a chain-length dependence of k_t^{st} has to be considered. For short chains, the α_s and i_c values determined for k_t^{ss} were assumed to hold also for k_t^{st}, as the center-of-mass diffusion properties of the coils should not be affected by the position of the free-radical site. For cross-termination of larger size SPRs with MCRs, $i > i_c$, the α_l value from recent Monte Carlo (MC) simulations was adopted.[52,53] This MC study suggests α_l to be in the range 0.16−0.27 depending on the degree of polymerization. Thus, an average value of $\alpha_l = 0.22$ was implemented for cross-termination, although values of 0.16 or 0.27 were also found to provide an adequate fit without having a significant effect on the other parameters. It should be noted that the chain length of the MCRs is poorly defined compared to the one of SPRs. Because of the slow propagation of MCRs, the correlation between time after the SP and radical size is lost. Chain length is thus only specified for SPRs.

The $c_{MCR}(t)$ curves are sensitive toward k_{bb} and $k_t^{st}(1,1)$ at relatively short times after laser pulsing, up to 0.2 s. This is because of the impact of high c_{SPR} on backbiting and cross-termination, respectively. The influence of k_p^t becomes important at longer times after pulsing. The rate coefficient for MCR homotermination, k_t^{tt}, was assumed to be given by the value derived from lumped parameters:[34] $k_t^{tt} = 9.0 \times 10^6 \exp[-674/(T/\text{K})]$ L mol^{-1} s^{-1}. Although MCR-MCR termination should go with a larger chain-length dependence, no α value is taken into account for the simple reason that MCR chain length is not specified and will certainly not be narrowly distributed.

The parameters c_R^0, $k_t^{ss}(1,1)$, $k_t^{st}(1,1)$, k_{bb}, and k_p^t were obtained by subjecting the experimental SPR and MCR concentration vs time traces to several cycles of PREDICI refinement. The close agreement between measured traces of both radical concentrations with the associated data from PREDICI simulation is illustrated in Figure 7 for 30 °C.

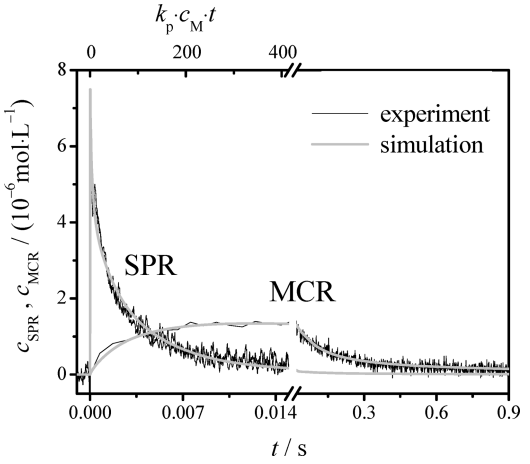

Figure 7. Experimental and simulated c_{SPR} and c_{MCR} vs time traces after single-pulse initiation, at $t = 0$, in BA solution polymerization (1.5 M in toluene) at 30 °C. The PREDICI simulation is based on the kinetics given in Scheme 1. The different time scales should be noted. They reflect the largely different reactivities of SPR and MCR species. The upper abscissa indicates SPR chain length after applying the laser single pulse at $t = 0$.

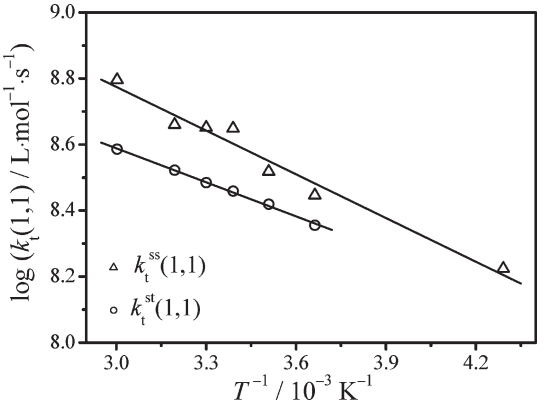

Figure 8. Temperature dependence of $k_t^{ss}(1,1)$ (triangles) and $k_t^{st}(1,1)$ (circles) as obtained by fitting of the SP-PLP-EPR. The Arrhenius straight lines correspond to activation energies of $E_a(k_t^{ss}(1,1)) = 8.4$ kJ mol^{-1} and $E_a(k_t^{st}(1,1)) = 6.6$ kJ mol^{-1}.

A discrepancy between calculated and measured SPR and MCR concentration vs time traces can only be seen in the very early time regime, up to 0.001 s after pulsing. This difference is assigned to a distortion of the EPR signal by the high-energy laser pulse.[40,51] This effect also accounts for the double maximum in c_{SPR} seen in Figure 3. Fitting of the SP-PLP-EPR data recorded at other temperatures in the range 0−60 °C may be accomplished with the same quality as shown for the 30 °C data in Figure 8. The procedure yields the Arrhenius parameters for $k_t^{ss}(1,1)$, $k_t^{st}(1,1)$, k_{bb}, and k_p^t, which are listed in Table 2.

The temperature dependence of $k_t^{ss}(1,1)$ and of $k_t^{st}(1,1)$ for polymerization of 1.5 M BA in toluene is shown in Figure 8. At identical temperature, the cross-termination rate coefficient, $k_t^{st}(1,1)$, is clearly below the rate coefficient for two SPRs of chain length unity, $k_t^{ss}(1,1)$. Because of uncertainties associated with the fitting procedure, the accuracy in the activation energies may be as large as ±2 kJ mol^{-1}, which says that the activation energies may be closer to each other

Table 2. Arrhenius Parameters for BA Polymerization Rate Coefficients Obtained via SP-PLP-EPR in the Present Study[a]

	pre-exponential factor/L mol^{-1} s^{-1} or s^{-1}	activation energy/ kJ mol^{-1}	k at 50 °C/L mol^{-1} s^{-1} or s^{-1}
$k_t^{ss}(1,1)$	1.3×10^{10}	8.4	5.7×10^8
$k_t^{st}(1,1)$	4.2×10^9	6.6	3.6×10^8
k_{bb}	1.6×10^8	34.7	3.9×10^2
k_p^t	9.2×10^5	28.3	25

[a] The data are obtained by Arrhenius fitting of individual rate coefficients for polymerization temperatures of 0, 10, 22, 30, 40, 50, and 60 °C; for deducing Arrhenius parameters of $k_t^{ss}(1,1)$, additional data from experiments at temperatures below 0 °C have been included; given in the last column of Table are rate coefficient values for 50 °C.

than is indicated by the slopes of the lines in Figure 8. They correspond to activation energies of $E_a(k_t^{ss}(1,1)) = 8.4$ kJ mol^{-1} and $E_a(k_t^{st}(1,1)) = 6.6$ kJ mol^{-1}. It should further be noted that the cross-termination rate coefficient is hypothetical in that no MCR of chain length unity may be envisaged. As it is unlikely that the Arrhenius lines for $k_t^{ss}(1,1)$ and $k_t^{st}(1,1)$ intersect each other, it appears reasonable to assume that both activation energies are close to each other and may be represented by the arithmetic mean of $E_a(k_t^{ss}(1,1))$ and $E_a(k_t^{st}(1,1))$: $E_a(k_t^s) = 7.5 \pm 2$ kJ mol^{-1}. The notation k_t^s indicates that both homo-termination of SPRs and cross-termination of an SPR and an MCR should be controlled by the reactivity of the SPR species.

Termination of short-chain radicals has recently been successfully analyzed in terms of center-of-mass diffusion.[40] The Smoluchowski equation for k_{diff} (eq 8) may be used together with the Stokes−Einstein relation (eq 9) for the mutual diffusion coefficient of radicals of chain length unity, $D_{1,1}$, for representation of $k_t(1,1) = k_{diff}$:

$$k_{diff} = 2\pi N_A D_{1,1} R_c \tag{8}$$

$$D_{1,1} = \frac{k_B T}{6\pi r_{1,1} \eta} \tag{9}$$

where N_A is Avogadro's number, R_c the effective capture radius, k_B Bolzmann's constant, and η the overall viscosity.

Combination of eq 8 and eq 9 indicates that the temperature dependence of the termination rate coefficient for two monomeric radicals is essentially given by $E_a(\eta^{-1})$, the activation energy of fluidity, as the capture radius and the hydrodynamic radius may be assumed to be constant. The temperature dependence of the fluidity of toluene, which is the main component (78 vol %) of the polymerizing medium, corresponds to an activation energy of $E_a(\eta^{-1}) = 8.9$ kJ mol^{-1}.[53] This number is remarkably close to $E_a(k_t^{ss}(1,1))$, but also to $E_a(k_t^s(1,1))$, which suggests that center-of-mass diffusion is controlling the termination rate of small radicals.

The crossover chain length of BA, $i_c \approx 30$, is in line with experimental results from SP-PLP-NIR-RAFT studies into the chain-length dependence of MA,[29] BA,[30] and DA[30] bulk homopolymerizations mostly carried out under high-pressure conditions, e.g., at 1000 bar. The values for i_c are in the range 20−30 with i_c being lowest for DA and largest for MA. For bulk polymerizations of methacrylates, such as dodecyl methacrylate,[38] cyclohexyl methacrylate,[38] benzyl methacrylate,[38] *n*-butyl methacrylate,[40] *tert*-butyl methacrylate,[40] and methyl methacrylate,[32] significantly higher i_c values were obtained by SP-PLP-EPR and, for methyl methacrylate, by RAFT-CLD-T.[52] Smaller i_c values around 50 are found with larger nonbranched methacrylates, such as *n*-butyl and dodecyl methacrylate, whereas the smallest member of the methacrylate family, MMA, exhibits an i_c value close to 100. These findings may be assigned to decreasing chain stiffness at larger size of the alkyl ester moiety. Chain entanglement and thus long-chain behavior occur at smaller chain length in the case of higher chain flexibility. It should be noted that glass-transition temperatures, which may be taken as some measure of chain stiffness, are significantly higher for methacrylates than for acrylates and increase toward smaller size of the alkyl ester moiety within the methacrylate family.

Table 3. Comparison of $k_t(1,1)$ Values for BA Radical Polymerization at 60 °C and 1 atm As Obtained by Various Experimental Techniques

$k_t(1,1)$/L mol^{-1} s^{-1} at 60 °C	experimental conditions	technique; ref
6.8×10^8	1.5 M toluene, 1 atm[a]	SP-PLP-EPR; this work
2×10^9	bulk, 1000 bar[b]	SP-PLP-NIR-RAFT; ref 30
1×10^9	bulk, 1 atm	RAFT-CLD-T; ref 30

[a] $k_t(1,1)$ extrapolated to 60 °C via the Arrhenius expression in Table 2. [b] $k_t(1,1)$ extrapolated to 1 atm via the activation volume: $\Delta V^{\ddagger} = -16$ cm^3 mol^{-1}.

Family type behavior is also seen for the short-chain-length exponent α_s. The numbers for methacrylates are in the range 0.50−0.65 with the larger values being found for linear nonbranched ester alkyl moieties. They are thus in the range which is to be expected on the basis of center-of-mass diffusion with constant capture radius for polymerization in "good" solvents and under theta conditions.[44−46] Pulsed-field-gradient NMR measurements of the diffusion coefficient of oligomeric MMA,[54] *n*-BMA,[54] and styrene[55] yield exponents of 0.66 for methacrylates and 0.51 for styrene exponents with the exponent referring to $D_i \sim i^{-\alpha}$.

For acrylate bulk polymerization, α_s has been determined by RAFT-assisted techniques to be well above the corresponding methacrylate numbers. For methyl acrylate and dodecyl acrylate, SP-PLP-NIR-RAFT studies resulted in α_s values of 0.78 and 1.12, respectively. For butyl acrylate, an ever higher value, $\alpha_s = 1.25$, was obtained via SP-PLP-NIR-RAFT and the RAFT-CLD-T method resulted in $\alpha_s = 1.04$. These α_s values are above what may be understood in terms of center-of-mass diffusion of small radical species and may be indicative of some impact of the RAFT agent on the kinetics in the early polymerization period. The BA short-chain exponent from SP-PLP-EPR, $\alpha_s = 0.85$, has the advantage of being situated in a reasonable range with the upper limit of $\alpha_s = 1$ referring to center-of-mass diffusion of rodlike species. High values of α_s have also been assigned to a more efficient shielding of the radical site during collision of small nonentangled radicals.[30,33,39] Along these lines, the more flexible acrylate chains would exhibit a more pronounced shielding than methacrylate oligomeric radicals of the same size.

The higher α_s for acrylates is associated with a smaller range of short-chain behavior; i.e., the crossover chain length of acrylates is significantly smaller than the one of methacrylates. As a consequence, a similar reduction, by about 1 order of magnitude, is seen between $k_t^{ss}(1,1)$ and $k_t(i_c,i_c)$. The latter quantity represents the k_t value at i_c, which is the chain length beyond which entanglement behavior occurs. The questions of whether and to which extent chain flexibility, shielding of the radical site and the shape of small diffusing radicals affect α_s can hopefully be answered as soon as further accurate composite-model parameters from SP-PLP-EPR become available. Another point to mention is that we found $k_t^{st}(1,1) \approx 0.5 k_t^{ss}(1,1)$, which agrees with the Smoluchowski model for translational diffusion by assuming a relative immobility of MCRs compared to SPRs.

Listed in Table 3 are $k_t(1,1)$ values for butyl acrylate polymerization as obtained by the three different techniques:

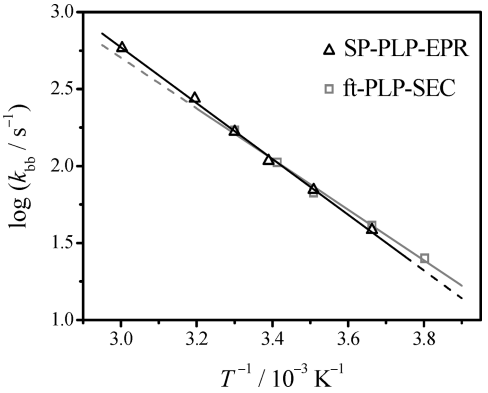

Figure 9. Comparison of backbiting rate coefficients, k_{bb}, obtained via SP-PLP-EPR (1.5 M BA in toluene) in the present study (black triangles) with literature data from frequency-tuned PLP-SEC[25] on BA bulk polymerization (gray squares). The black and gray lines represent Arrhenius fits to the individual data.

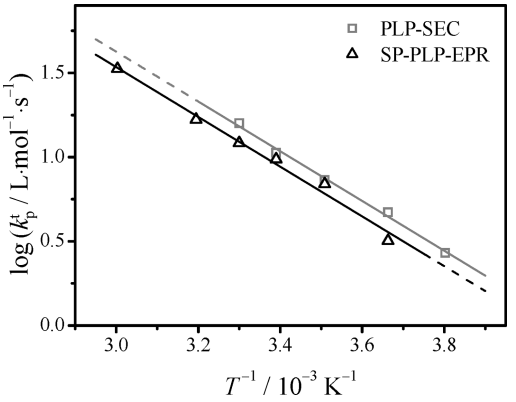

Figure 10. Temperature dependence of the propagation rate coefficient of the tertiary midchain radical, k_p^t, determined from the present SP-PLP-EPR study for BA polymerization (1.5 M in toluene) (black triangles) and k_p^t from PLP-SEC under variation of laser repetition rate in bulk (gray squares).[25] Arrhenius fitting is indicated by the black and gray lines. From the slope of the individual Arrhenius lines fitted to the SP-PLP-EPR and PLP-SEC data, activation energies of 28.3 and 28.9 kJ mol^{-1}, respectively, are obtained.

SP-PLP-EPR, SP-PLP-NIR-RAFT, and RAFT-CLD-T. The two RAFT-mediated studies have been carried out on bulk polymerization, whereas the novel SP-PLP-EPR method has been applied to BA dissolved in toluene. It should be stressed that $k_t(1,1)$ from SP-PLP-EPR refers to the well-defined quantity $k_t^{ss}(1,1)$, whereas the $k_t(1,1)$ numbers from RAFT-assisted techniques are composed of contributions of $k_t^{ss}(1,1)$ and $k_t^{st}(1,1)$.

Although the distribution of SPRs and MCRs may be different in these experiments, the data in Table 3 seem to indicate that $k_t(1,1)$ is not significantly dependent on the specific technique applied for measurement or on solvent environment. The close similarity between the bulk and solution $k_t(1,1)$ data may be due to the viscosity of pure BA not being too different from the one of the BA−toluene mixture. The size of $k_t(1,1)$ seems to reflect, at least partly, the differences in the associated short-chain exponent α_s. A larger α_s goes with larger $k_t(1,1)$.

The backbiting rate coefficients, k_{bb}, which were obtained by the PREDICI modeling of SP-PLP-EPR data, are plotted in Figure 9 together with the k_{bb} values deduced via the frequency-tuned PLP-SEC method.[25]

Both data sets, obtained from different experimental approaches, closely overlap, which provides strong evidence for the high accuracy of both techniques. Moreover, this imparts some benchmark character to the k_{bb} data. The Arrhenius parameters from SP-PLP-EPR of $E_a(k_{bb}) = 34.7 \pm 0.8$ kJ mol^{-1} and $A(k_{bb}) = (1.6 \pm 0.7) \times 10^8$ s^{-1} are close to the ones obtained from the PLP-SEC data of $E_a(k_{bb}) = 31.7 \pm 2.5$ kJ mol^{-1} and $A(k_{bb}) = (4.84 \pm 0.29) \times 10^7$ s^{-1}. Linear fitting of the joint $\log(k_{bb})$ vs T^{-1} data results in $E_a(k_{bb}) = 33.3 \pm 0.7$ kJ mol^{-1} and $A(k_{bb}) = (9.3 \pm 2.9) \times 10^7$ s^{-1}. The data depicted in Figure 9 may also be compared with values for k_{bb} obtained for BA bulk polymerization from the polymer branching level determined via ^{13}C NMR spectroscopy.[27] Because of the lower sensitivity of ^{13}C NMR spectroscopy, these k_{bb} values show a significantly larger scatter and partially are by up to a factor of 2 above the data in Figure 9.

The temperature dependencies of k_p^t for polymerization of BA determined via SP-PLP-EPR and via PLP-SEC are shown in Figure 10. Taking experimental accuracy into account, the activation energy from SP-PLP-EPR, $E_a(k_p^t) = 28.3 \pm 1.7$ kJ mol^{-1}, is identical to the one from ft-PLP-SEC, $E_a(k_p^t) = 28.9 \pm 3.2$ kJ mol^{-1}. However, the pre-exponential factor of $A(k_p^t) = (9.2 \pm 6.3) \times 10^5$ L mol^{-1} s^{-1} from SP-PLP-EPR is slightly below the PLP-SEC value of $A(k_p^t) = (1.52 \pm 0.14) \times 10^6$ L mol^{-1} s^{-1}, although still in agreement within the limits of uncertainty. The reason for the discrepancy in pre-exponential factor by about 30% may be due to SEC calibration or to an uncertainty in conversion detection, which affects the k_p^t value that is deduced from the product $k_p^t c_M$ in the simulation of the SP-PLP-EPR data. An intrinsic kinetic effect may occur in that k_p^t in toluene differs from k_p^t in bulk.[56] At present, it cannot be decided which experimental technique provides the more accurate k_p^t. Fitting the combined k_p^t data set with the average activation energy of $E_a(k_p^t) = 28.6$ kJ mol^{-1} yields the Arrhenius expression: $k_p^t = 1.17 \times 10^6 \exp[-3440/(T/K)]$ L mol^{-1} s^{-1}.

Conclusion

The evolution of secondary propagating radicals (SPRs) and tertiary midchain radicals (MCRs) after laser-pulse-induced production of an intense burst of photoinitiator-derived radicals has been monitored by EPR spectroscopy with a time resolution of about 0.1 ms. Butyl acrylate (BA) radical polymerization in solution of toluene has been studied at ambient pressure and temperatures between −40 and 60 °C. At −40 °C, the backbiting reaction, which transforms SPR into MCR species, via 1,5-hydrogen shift, occurs only to a marginal extent. Hence, the rate coefficient for homo-termination of SPRs may be determined without the interference of MCRs. The SPR termination kinetics may be adequately represented by the composite model for chain-length-dependent k_t. Above 0 °C both types of radicals are monitored after single pulse initiation. The so-obtained radical concentration vs time traces allow for the determination of the Arrhenius parameters for homotermination of two SPRs, $k_t^{ss}(i,i)$, cross-termination between an SPR and an MCR, $k_t^{st}(i,i)$, backbiting, k_{bb}, and propagation of an MCR, k_p^t. The k_{bb} and k_p^t values from SP-PLP-EPR are in very close agreement with literature data from frequency-tuned PLP-SEC.[25] The backbiting rate coefficients from SP-PLP-EPR are slightly below the k_{bb} data deduced from polymer branching levels via ^{13}C NMR.[27] The composite-model parameters $k_t(1,1)$, i_c, and α_l for SPRs from SP-PLP-EPR are in close agreement with literature data[28−30,32,33] derived from rate coefficients averaged over termination reactions of secondary and tertiary radicals. The exponent $\alpha_s = 0.85$, which characterizes the chain-length dependence of k_t^{ss} within the regime of short chains, is appreciably below the

numbers deduced from RAFT-assisted techniques but appears to be of reasonable size.

The direct quantitative detection of different types of relevant radical species by SP-PLP-EPR should afford for very detailed investigations into the kinetics of both conventional and controlled radical polymerization.

Acknowledgment. Financial support by the Deutsche Forschungsgemeinschaft within the European Graduate School "Microstructural Control in Free-Radical Polymerization" (GRK 585) and a fellowship from the Fonds der Chemischen Industrie (to J.B.) are gratefully acknowledged. The authors are grateful to Prof. F. Meyer (Institute for Inorganic Chemistry, University of Göttingen) for providing the opportunity of using the EPR spectrometer in his laboratory.

References and Notes

(1) Junkers, T.; Barner-Kowollik, C. *J. Polym. Sci., Polym. Chem.* **2008**, *46*, 7585–7605.
(2) Scott, G. E.; Senogles, E. *J. Macromol. Sci.* **1970**, *A 4*, 1105–1117.
(3) Scott, G. E.; Senogles, E. *J. Macromol. Sci.* **1973**, *C 9*, 49–69.
(4) Scott, G. E.; Senogles, E. *J. Macromol. Sci.* **1974**, *A 8*, 753–773.
(5) Wunderlich, W. *Makromol. Chem.* **1976**, *177*, 973–989.
(6) Madruga, E. L.; Fernandez-Garcia, M. *Macromol. Chem. Phys.* **1996**, *197*, 3743–3755.
(7) McKenna, T. F.; Villanueva, A.; Santos, A. M. *J. Polym. Sci., Polym. Chem.* **1999**, *37*, 571–588.
(8) Fernandez-Garcia, M.; Fernandez-Sanz, M.; Madruga, E. L. *Macromol. Chem. Phys.* **2000**, *201*, 1840–1845.
(9) Olaj, O. F.; Bitai, I.; Hinkelmann, F. *Makromol. Chem.* **1987**, *188*, 1689–1702.
(10) Beuermann, S.; Buback, M.; Davis, T. P.; Gilbert, R. G.; Hutchinson, R. A.; Olaj, O. F.; Russell, G. T.; Schweer, J.; van Herk, A. M. *Macromol. Chem. Phys.* **1997**, *198*, 1545–1560.
(11) Asua, J. M.; Beuermann, S.; Buback, M.; Castignolles, P.; Charleux, B.; Gilbert, R. G.; Hutchinson, R. A.; Leiza, J. R.; Nikitin, A. N.; Vairon, J. P.; van Herk, A. M. *Macromol. Chem. Phys.* **2004**, *205*, 2151–2160.
(12) Barner-Kowollik, C.; Günzler, F.; Junkers, T. *Macromolecules* **2008**, *41*, 8971–8973.
(13) Willemse, R. X. E.; van Herk, A. M.; Panchenko, E.; Junkers, T.; Buback, M. *Macromolecules* **2005**, *38*, 5098–5103.
(14) Nikitin, A. N.; Hutchinson, R. A. *Macromolecules* **2005**, *38*, 1581–1590.
(15) Barth, J.; Buback, M. *Macromol. React. Eng.* **2010**, *4*, DOI: 10.1002/mren.200900066.
(16) Roedel, M. J. *J. Am. Chem. Soc.* **1953**, *75*, 6110–6112.
(17) Toh, J. S. S.; Huang, D. M.; Lovell, P. A.; Gilbert, R. G. *Polymer* **2001**, *42*, 1915–1920.
(18) Kajiwara, A. *ACS Symp. Ser.* **2006**, *944*, 111–124.
(19) Kajiwara, A. *Macromol. Symp.* **2007**, *248*, 50–59.
(20) Kajiwara, A.; Kamachi, M. *ACS Symp. Ser.* **2003**, *854*, 86–100.
(21) Kajiwara, A.; Nanda, A. K.; Matyjaszewski, K. *Macromolecules* **2004**, *37*, 1378–1385.
(22) Barth, J.; Buback, M.; Hesse, P.; Sergeeva, T. *Macromol. Rapid Commun.* **2009**, *30*, 1969–1974.
(23) Boschmann, D.; Vana, P. *Macromolecules* **2007**, *40*, 2683–2693.
(24) Farcet, C.; Belleney, J.; Charleux, B.; Pirri, R. *Macromolecules* **2002**, *35*, 4912–4918.
(25) Nikitin, A. N.; Hutchinson, R. A.; Buback, M.; Hesse, P. *Macromolecules* **2007**, *40*, 8631–8641.
(26) Plessis, C.; Arzamendi, G.; Leiza, J. R.; Schoonbrood, H. A. S.; Charmot, D.; Asua, J. M. *Macromolecules* **2000**, *33*, 5041–5047.
(27) Plessis, C.; Arzamendi, G.; Alberdi, J. M.; van Herk, A. M.; Leiza, J. R.; Asua, J. M. *Macromol. Rapid Commun.* **2003**, *24*, 173–177.
(28) Buback, M.; Junkers, T.; Vana, P. *Macromol. Rapid Commun.* **2005**, *26*, 796–802.
(29) Buback, M.; Hesse, P.; Junkers, T.; Theis, T.; Vana, P. *Aust. J. Chem.* **2007**, *60*, 779–787.
(30) Junkers, T.; Theis, A.; Buback, M.; Davis, T. P.; Stenzel, M. H.; Vana, P.; Barner-Kowollik, C. *Macromolecules* **2005**, *38*, 9497–9508.
(31) Vana, P.; Davis, T. P.; Barner-Kowollik, C. *Macromol. Rapid Commun.* **2002**, *23*, 952–956.
(32) Johnston-Hall, G.; Theis, A.; Monteiro, M. J.; Davis, T. P.; Stenzel, M. H.; Barner-Kowollik, C. *Macromol. Chem. Phys.* **2005**, *206*, 2047–2053.
(33) Theis, A.; Feldermann, A.; Charton, N.; Davis, T. P.; Stenzel, M. H.; Barner-Kowollik, C. *Polymer* **2005**, *46*, 6797–6809.
(34) Nikitin, A. N.; Hutchinson, R. A. *Macromol. Theory Simul.* **2006**, *15*, 128–136.
(35) Kaszas, G.; Foldesberezsnich, T.; Tudos, F. *Eur. Polym. J.* **1983**, *19*, 469–473.
(36) Beuermann, S.; Buback, M. *Prog. Polym. Sci.* **2002**, *27*, 191–254.
(37) Buback, M.; Egorov, M.; Junkers, T.; Panchenko, E. *Macromol. Rapid Commun.* **2004**, *25*, 1004–1009.
(38) Buback, M.; Müller, E.; Russell, G. T. *J. Phys. Chem. A* **2006**, *110*, 3222–3230.
(39) Buback, M.; Egorov, M.; Junkers, T.; Panchenko, E. *Macromol. Chem. Phys.* **2005**, *206*, 333–341.
(40) Barth, J.; Buback, M.; Hesse, P.; Sergeeva, T. *Macromolecules* **2009**, *42*, 481–488.
(41) Barth, J.; Buback, M. *Macromol. Rapid Commun.* **2009**, *30*, 1805–1811.
(42) Smith, G. B.; Russell, G. T.; Heuts, J. P. A. *Macromol. Theory Simul.* **2003**, *12*, 299–314.
(43) Smith, G. B.; Russell, G. T. *Z. Phys. Chem.* (*Munich*) **2005**, *219*, 295.
(44) Mahabadi, H. K.; O'Driscoll, K. F. *J. Polym. Sci., Polym. Chem.* **1977**, *15*, 283–300.
(45) Mahabadi, H. K.; O'Driscoll, K. F. *Macromolecules* **1977**, *10*, 55–58.
(46) Flory, P. J. *Principles of Polymer Chemistry*; Cornell University Press: Ithaca, NY, 1953.
(47) Friedman, B.; O'Shaughnessy, B. *Macromolecules* **1993**, *26*, 5726–5739.
(48) Khokhlov, A. R. *Macromol. Chem., Rapid Commun.* **1981**, *2*, 633–636.
(49) Olaj, O. F.; Zifferer, G. *Makromol. Chem., Rapid Commun.* **1982**, *3*, 549–556.
(50) Buback, M.; Hesse, P.; Junkers, T.; Sergeeva, T.; Theis, T. *Macromolecules* **2008**, *41*, 288–291.
(51) Forbes, M. D. E. *Photochem. Photobiol.* **1997**, *65*, 73–81.
(52) Barner-Kowollik, C.; Russell, G. T. *Prog. Polym. Sci.* **2009**, *34*, 1211–1259.
(53) Harris, K. R. *J. Chem. Eng. Data* **2000**, *45*, 893–897.
(54) Griffiths, M. C.; Strauch, J.; Monteiro, M. J.; Gilbert, R. G. *Macromolecules* **1998**, *31*, 7835–7844.
(55) Piton, M. C.; Gilbert, R. G.; Chapman, B. E.; Kuchel, P. W. *Macromolecules* **1993**, *26*, 4472–4477.
(56) Beuermann, S. *Macromol. Rapid Commun.* **2009**, *30*, 1066–1088.